

Submitted to *INFORMS Journal on Computing*

Learn to formulate: A surrogate model framework for generalized assignment problem with routing constraints

Sen Xue, Chuanhou Gao

School of Mathematical Sciences, Zhejiang University, Hangzhou, China, senx@zju.edu.cn, gaochou@zju.edu.cn

Authors are encouraged to submit new papers to INFORMS journals by means of a style file template, which includes the journal title. However, use of a template does not certify that the paper has been accepted for publication in the named journal. INFORMS journal templates are for the exclusive purpose of submitting to an INFORMS journal and are not intended to be a true representation of the article's final published form. Use of this template to distribute papers in print or online or to submit papers to another non-INFORM publication is prohibited.

Abstract. The generalized assignment problem with routing constraints, e.g. the vehicle routing problem, has essential practical relevance. This paper focuses on addressing the complexities of the problem by learning a surrogate model with reduced variables and reconstructed constraints. A surrogate model framework is presented with a class of surrogate models and a learning method to acquire parameters. The paper further provides theoretical results regarding the representational power and statistical properties to explore the effectiveness of this framework. Numerical experiments based on two practical problem classes demonstrate the accuracy and efficiency of the framework. The resulting surrogate models perform comparably to or surpass the state-of-the-art heuristics on average. Our findings provide empirical evidence for the effectiveness of utilizing size-reduced and reconstructed surrogate models in producing high-quality solutions.

Key words: Integer programming; Artificial intelligence; Transportation-shipping;

1. Introduction

The generalized assignment problem (GAP) is a fundamental model in combinatorial optimization. It requires the determination of an optimal allocation of tasks to agents while adhering to knapsack constraints. This problem bears significant practical relevance across a broad range of industrial contexts (Pentico 2007). For instance, in the logistics field, a basic concern is to properly allocate a set of orders to distinct vehicles for shipping. Additional applications have been developed in foundational studies on scheduling (Aringhieri et al. 2015, Cacchiani and Salazar-González 2017, Boccia et al. 2023), production planning (Benjaafar et al. 2004, Dobson and Nambimadom 2001), and location problems (Fischetti et al. 2016, Mikić et al. 2019).

Many applications are formulated based on the GAP with additional routing constraints for practical needs. In this study, we specifically define these GAP-based problems as the generalized assignment problem with routing constraints (GAPR), and detail this definition in subsequent sections. A common example

is the capacitated vehicle routing problem (CVRP) and its variants. This integration necessitates the inclusion of further constraints and variables to address practical considerations, such as path distance or delivery time windows. A similar scenario is observed in warehouse management, where orders are grouped into batches and picked from their respective storage locations. According to Bartholdi and Hackman (2014), these operations account for 55% of the overall warehouse expenses. Recent studies increasingly investigate the inclusion of sequential picker routing in joint modeling (Aerts et al. 2021, Zhang and Gao 2023). This integration reportedly yields more cost reduction in practical outcomes than focusing on single processes (Won and Olafsson* 2005). Other integrated problems can be found in studies by Matusiak et al. (2017), Yadav and Tanksale (2022). Consequently, these extended problems demand more complex models with increasing challenges for solutions. It further raises the challenge of solving efficiency, which is a vital measure of practicality.

Reviews on related problems show that manually designed and customized heuristics are the most widely used for the GAPR, with exact approaches being the minority (Pardo et al. 2024, Gutiérrez-Sánchez and Rocha-Medina 2022). Exact approaches are superior in small-scale problems but are limited by the exponential growth of model size. Moreover, machine learning (ML) methods are widely integrated into optimization methods for effective problem-solving, such as branching strategy (Khalil et al. 2016, Gasse et al. 2019), cutting plane selection (Paulus et al. 2022), and large neighborhood search (Wu et al. 2021). However, little research considers the modification of the formulation structure, which might be more fundamental. This relatively leaves a gap for our study.

In this paper, we introduce a general-purpose learning framework to directly approximate the GAPR formulations. Considering the extensive diversity of routing constraints depending on reality needs, this approach highlights its advantages by automatically learning and solving without requiring problem-specific algorithm designation. Our purpose differs from the traditional exact approach that seeks a refined and tightened formulation while maintaining all necessary constraints. This approach involves the reduction of variables and the reconstruction of constraints. Supporting evidence and motivation are found in studies on branching strategies (Khalil et al. 2016, Gasse et al. 2019), where fewer branching nodes usually indicate less search time within the branch-and-bound (B&B) tree. Therefore, by implementing a model with fewer integer variables, the B&B tree might be significantly reduced. Consequently, the resultant closely-approximated model of the GAPR can be expected to produce near-optimal solutions more efficiently.

1.1. Literature review

The topic of learning to optimize (L2O) has attracted increasing attention in recent years. Our discussion focuses on the works on L2O related to mixed integer programming (MIP) optimization. Notably, studies by Zhang et al. (2023), Karimi-Mamaghan et al. (2022) and Bengio et al. (2021) have investigated comprehensive reviews. A common purpose is to accelerate the MIP problem-solving process. To fulfill this purpose,

parameterized ML models are trained to replace either parts or the entire computationally expensive algorithms. A representative application is the designate of the branching strategy within the B&B algorithm. Studies by Khalil et al. (2016) and Gasse et al. (2019) utilized ML models to imitate the strong branching strategy, which is an exact one-step look-ahead strategy, with a high computational cost. This approximation allows a close high performance while significantly reducing the computational time required.

However, relatively few studies concern the formulation of MIP. An aspect highlighted within these studies is that certain constraints or the objective function are not explicit. To address this issue, ML techniques are employed to approximate these undefined elements. Subsequently, the approximation ML models are embedded or integrated into the MIP formulation for further optimization. The resultant MIP models can also be referred to as surrogate models in response to the true models that cannot be explicitly expressed. Notably, Schweidtmann et al. (2022) and Fajemisin et al. (2023) have provided comprehensive overviews on the topic as *constraint learning* but with a wider range of continuous and discrete optimization problems. We discuss the MIP-related works based on their ML methods.

The regression or linear approximation functions are widely used to construct MIP formulations. This method is extensively utilized in engineering with first- and second-order polynomials. Take the work by Bertsimas et al. (2016) as an example. This modeling approach is widely recognized for its directness and efficiency. Kleijnen (2018) presented an overview.

The tree ensembles are popular tools for constraint learning. Research conducted by Biggs et al. (2017) and Mišić (2020) has introduced general frameworks that enable the representation of tree ensembles within MIP formulations. The applications of tree ensembles for optimization include the investigation of the electricity network problem (Gutina et al. 2023) and the optimal power flow problem (Halilbašić et al. 2018). Tree ensembles are valued for their interpretability for analysis and practice purposes (Fajemisin et al. 2023). However, the complexity of representing decision trees is a function of the tree size, making the resolution challenging with the growth of the tree. Mišić (2020) proposed a Benders decomposition method for efficient problem-solving. Concurrently, the study by Mistry et al. (2021) provided a branch-and-cut (B&C) algorithm with specific branching rules.

The utilization of neural networks is another widespread approach for generating learned models. The study by Fischetti and Jo (2018) initially proposed that both deep neural networks and convolutional neural networks could be presented as MIP formulations. Recent applications include the optimization of chemical processes (Zhou et al. 2024), the optimal power flow problem (Kilwein et al. 2023), and the task scheduling problem (Rigo et al. 2023). The embedding of neural networks is also challenged by the large size and solving difficulty of the resultant MIP formulation (Fajemisin et al. 2023). To address this issue, Grimstad and Andersson (2019) introduced bound-tightening algorithms to refine the values within the big-M constraints. Anderson et al. (2020) proposed valid inequalities to strengthen the MIP formulations. Further, Wang et al. (2023) utilized a Lagrangian relaxation-based B&C procedure to produce higher-quality solutions.

Our study could provide a new perspective for L2O research. Firstly, most L2O studies, which focus on acceleration, rely on pre-established models with large feasible solution space. The resultant improvements might be therefore inherently limited. In contrast, our approach modifies and simplifies the formulations, leading to reduced search space and potential further improvements in efficiency. Secondly, many ML-based methods encounter obstacles in solving speed, necessitating further optimization efforts. A possible reason might be that the ML techniques are initially built for general learning tasks, without adaptations for the optimization of their embedded models. Our framework is specifically designed with elements of GAPR, allowing for optimization without additional modifications. To the best of our knowledge, no study has been conducted on learning-based formulation modification on generalized assignment problems.

1.2. Contributions and structure

Our contributions in this paper are listed as follows:

1. We present a direct approximation framework with a class of surrogate models and a learning method for the efficient problem-solving of the GAPR.
2. We provide theoretical results on the effectiveness of our framework on aspects of learning capacity and statistical analysis.
3. We demonstrate the efficacy of the framework by conducting numerical experiments on two classes of the GAPR of practical relevance.

This paper is structured as follows. Section 2 presents a description and general formulations of the GAPR. Section 3 introduces our methodology to maintain a size-reduced and reconstructed surrogate model. Section 4 provides theoretical results of the representational power and statistical properties of our framework. Section 5 examines our approach comparing the exact algorithms. Finally, Section 6 summarizes the study and outlines future research directions.

2. Problem description

We consider the GAPR as a problem of finding the optimal task assignment and route selection that minimizes both the allocation and transportation costs. Denote a set of tasks as I and a set of agents as J . Consider a graph G , where one of its nodes serves as the depot. Each task corresponds to one or more nodes in G . Once a task is assigned to an agent, the agent must visit its corresponding nodes in G from the depot with routing constraints, such as subroute elimination and soft time windows.

Following the description of the GAPR, we provide a general MIP formulation. Suppose that task $i \in I$ weights w_i . The capacity of an agent j is Q_j . Denote y_{ij} as a binary variable for determining the assignment of task $i \in I$ to agent $j \in J$, where $y_{ij} = 1$ indicates that task i is assigned to agent j , and $y_{ij} = 0$ otherwise. Let $y = (y_{11}, y_{12}, \dots, y_{ij}, \dots, y_{|I||J|})$. Due to the absence of predefined routing rules, we denote the remaining variables as $u \in \mathbb{R}^m \times \mathbb{Z}^n$ with domain of D_u and constraints coefficients as matrices $B \in \mathbb{R}^{r \times |I||J|}$,

$E \in \mathbb{R}^{r \times m \times n}$ and $e \in \mathbb{R}^r$. Here m , n , and r are arbitrary positive integers. The GAPR can be formulated as follows.

$$\min \quad c^\top y + d^\top u \quad (1a)$$

$$\text{s.t.} \quad \sum_{j \in J} y_{ij} = 1, \quad \forall i \in I; \quad (1b)$$

$$\sum_{i \in I} w_i y_{ij} \leq Q_j, \quad \forall j \in J; \quad (1c)$$

$$\sum_{i \in I} y_{ij} \geq 1, \quad \forall j \in J^*; \quad (1d)$$

$$By + Eu \leq e, \quad (1e)$$

$$y_{ij} \in \{0, 1\}, \quad \forall i \in I, \forall j \in J; \quad (1f)$$

$$u \in D_u \cap (\mathbb{R}^m \times \mathbb{Z}^n); \quad (1g)$$

Here the objective function is computed as the assignment cost $c^\top y$ and routing cost $d^\top u$. Constraints (1b) ensure that each task is uniquely assigned to an agent. Constraints (1c) guarantee that the assignment does not exceed the capacity of the agents. In certain scenarios where no agent should remain unassigned, this condition is expressed by constraints (1d) with the notation $J^* = J$. In cases where such a requirement is not applicable, we set $J = \emptyset$. All routing constraints are denoted by constraints (1e). Finally, the variable domains are defined by constraints (1f) and (1g).

We further introduce two assumptions for the GAPR. Firstly, agents are assumed to be homogeneous, implying that capacity limits Q_j are uniformly denoted by Q across all agents. Secondly, let y^* be an integer solution, representing an assignment plan, that satisfies constraints (1b), (1c), (1d) and (1f). We assume then there exists a feasible u^* corresponding to y^* that satisfies the constraints (1e) and (1g). The assumption proposes that any assignment being feasible to the GAP constraints is at least feasible to the routing constraints. This assumption still covers most CVRP variants and order batching problems. In certain scenarios such as hard time windows, assignments could be infeasible due to routing constraints. However, early-stage studies have indicated that the hard time windows can be reformulated into soft constraints by incorporating appropriate penalties on these infeasible solutions (Taillard et al. 1997).

The objective value of the GAPR model can then be represented as a function of y with the assumptions above, providing a learning target. Initially, we define the feasible region of y as P under the assignment and knapsack constraints, thereby also feasible to the GAPR as assumed.

$$P = \{y : (1b), (1c), (1d), (1f)\}. \quad (2)$$

Therefore, the objective value can be presented as a function to minimize the remaining variables u with given \hat{y} as follows:

$$f_{\text{obj}}(\hat{y}) = \min_u \{c^\top y + \lambda^\top u : y = \hat{y}, (1b), (1c), (1d), (1e), (1f), (1g)\}. \quad (3)$$

Finally, the task to minimize the GAPR model can be proposed as an optimization problem on $f_{\text{obj}}(y)$:

$$\min_{y \in P} f_{\text{obj}}(y), \quad (4)$$

as y denotes integer points in P . In subsequent sections, we study surrogate models to approximate $f_{\text{obj}}(y)$. The surrogate models are designed with significantly reduced computational demands. As a result, the models might quickly produce near-optimal solutions of the original GAPR model, thereby offering a practical approach to solving the GAPR optimization problem.

3. Methodology

In this section, we introduce our methodology. Initially, we formulate a specific class of surrogate models, starting with their motivation from heuristic principles. Subsequently, we introduce the learning framework, including algorithms for sampling, regression, and iterative training.

3.1. Surrogate model

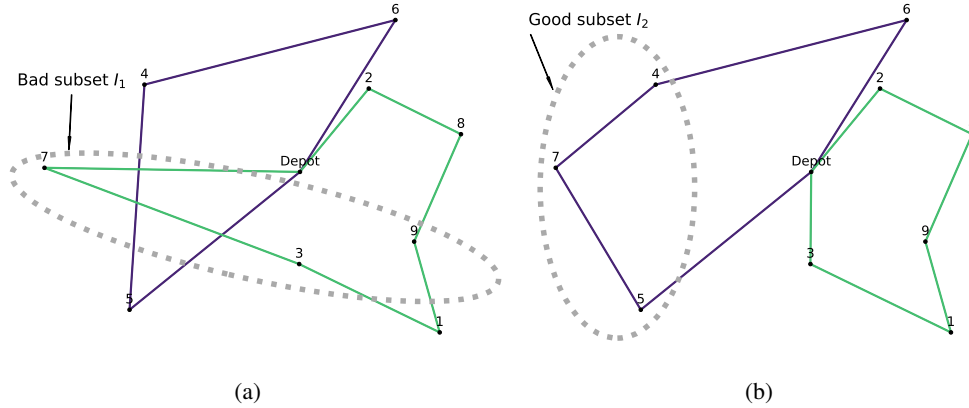
3.1.1. Motivation from neighborhood search The development of our surrogate model is motivated by the neighborhood search (NS) strategies utilized for assignment problems. These strategies typically function by partially destroying and reconstructing a solution, while evaluating the potential improvement of such modifications. Within the context of the GAPR, we first delineate a feasible assignment as a sequence of subsets drawn from the set of tasks I , stated as follows:

$$s = (s^k)_{k \in J}, \quad s^k \subset I \quad \forall k \in J. \quad (5)$$

Here each s^k represents a subset of I satisfying $\bigcup_{k \in J} s^k = I$, capacity constraints, and $s^{k_1} \cap s^{k_2} = \emptyset$ for two distinct $k_1, k_2 \in J$. The NS strategies would modify parts of the solution s through operations such as swapping and reallocation. To illustrate this process, we present a CVRP instance of 9 customers with different assignment and routing paths in Figure 1 as an example. In this instance, The strategies may identify subset I_1 in Figure (1a) as a reason for bad performance as it initially allocates highly dispersed nodes along the same route. Conversely, The strategies may recognize I_2 in Figure (1b) as an alternative good subset as it gathers closely located neighbors, indicating a lower routing distance. Given these considerations, a solution incorporating I_1 could be converted into one containing I_2 by reallocating node 7 to be with nodes 4 and 5.

However, if we could identify the good subsets in advance, the process can be transformed into a problem-solving procedure to find near-optimal solutions that contain routes including these good subsets. Denote the set of all nonempty subsets of I as $\mathcal{P}^*(I)$. For example, if $I = \{1, 2, 3\}$, then $\mathcal{P}^*(I) =$

Figure 1 A CVRP instance with two vehicles



$\{\{1\}, \{2\}, \{3\}, \{1, 2\}, \{2, 3\}, \{1, 3\}, \{1, 2, 3\}\}$. Define H as a subset of indices of $\mathcal{P}^*(I)$, where each element corresponds to a subset of I denoted as I_η for each $\eta \in H$. The problem of finding solutions with identified good subsets can be stated as follows.

Problem: For a given set H , find a feasible s ensuring for any $\eta \in H$,
 there exists $k \in J$ such that $I_\eta \subseteq s^k$. (P1)

The problem (P1) might produce some initially near-optimal solutions if H is properly selected. To further explore this problem, we define a function g_H with a given set H as follows:

$$g_H(s) = \sum_{\eta \in H} \sum_{k \in J} \mathbf{1}_{I_\eta \cap s^k \neq \emptyset}. \quad (6)$$

Here $\mathbf{1}_{I_\eta \cap s^k \neq \emptyset}$ is a binary activation function that returns 1 if $I_\eta \cap s^k$ is nonempty and 0 otherwise. We propose the following proposition describing the relationship between g_H and problem (P1).

PROPOSITION 1. *Let I denote a set of tasks and H a set of indices of $\mathcal{P}^*(I)$. Assume problem (P1) is feasible. Then a feasible assignment plan \hat{s} is a solution to problem (P1) if and only if $g_H(\hat{s}) = |H|$.*

Proof. Consider two assertions to establish the necessary and sufficient conditions.

First, assume \hat{s} is indeed a solution to (P1). Under this assumption, each subset I_η , for $\eta \in H$, is exclusively allocated to a specific $\hat{s}^{k(\eta)}$, denoting $k(\eta)$ is the corresponding subset in s to η . This allocation implies that for any other index $k \neq k(\eta)$, the intersection $I_\eta \cap \hat{s}^k$ is empty. Consequently, the function g_H evaluated at \hat{s} can be expressed as:

$$g_H(\hat{s}) = \sum_{\eta \in H} \sum_{k \in J} \mathbf{1}_{I_\eta \cap \hat{s}^k \neq \emptyset} = \sum_{\eta \in H} 1 = |H|. \quad (7)$$

Second, assume the condition $g_H(\hat{s}) = |H|$ holds. Given that no I_η is empty, it follows that for any $\eta \in H$, the sum $\sum_{k \in J} \mathbf{1}_{I_\eta \cap \hat{s}^k \neq \emptyset} \geq 1$. Hence, we deduce that this sum equals exactly 1 for every $\eta \in H$. This

conclusion implies that each task subset I_η is uniquely allocated to one subset \hat{s}^k . Therefore, \hat{s} satisfies the exclusive allocation requirement for being a solution to **(P1)**.

The proposition 1 delineates an equivalence condition wherein an assignment plan s is identified as a solution for the problem **(P1)**. Additionally, it can be found that for any s , $g_H(s) \geq \sum_{\eta \in H} 1 = |H|$, since there is always at least one subset in s contains elements in a given I_η . Consequently, it enables the reformulation of **(P1)** into an optimization problem as $\min g_H(s)$, where s denotes all feasible solutions. In the following context, we explore the property of this optimization problem in detail.

3.1.2. Set indicator surrogate model We introduce an optimizable surrogate model that frames problem **(P1)** as a minimization task. Initially, we delineate the relationship between the variables y in the model(1) and the assignment plans s as the following observation.

OBSERVATION 1. Let I denote a set of tasks and P the polyhedron of feasible integers in equation (2). The feasible assignment plans s are in one-to-one correspondence to the feasible points y in P . By Observation 1, we can denote the corresponding \hat{y} to a specific \hat{s} as $\hat{s} = s(\hat{y})$ and $\hat{y} = y(\hat{s})$ conversely. We can propose problem **(P1)** as the following optimization problem:

$$\min_{y \in P} g_H(s(y)). \quad (8)$$

Problem (8) can be further included in the following set indicator model:

$$\min \sum_{\eta \in H} \beta_\eta \left(\sum_{j \in J} \delta_{j\eta} \right) \quad (9a)$$

$$\text{s.t. } \sum_{j \in J} y_{ij} = 1, \quad \forall i \in I; \quad (9b)$$

$$\sum_{i \in I} w_i y_{ij} \leq Q, \quad \forall j \in J; \quad (9c)$$

$$\sum_{i \in I} y_{ij} \geq 1, \quad \forall j \in J^*; \quad (9d)$$

$$M_\eta \delta_{j\eta} \geq \sum_{i \in I_\eta} y_{ij}, \quad \forall j \in J, \quad \forall \eta \in H; \quad (9e)$$

$$y_{ij} \in \{0, 1\}, \quad \forall i \in I, \quad \forall j \in J; \quad (9f)$$

$$\delta_{j\eta} \in \{0, 1\}, \quad \forall j \in J, \quad \forall \eta \in H; \quad (9g)$$

Here $\beta_\eta \in \mathbb{R}$ and $M_\eta = |I_\eta|$ for all $\eta \in H$. Constraints (9b)-(9d) are the same with Constraints (1b)-(1d). The big-M constraints (9e) make variables $\delta_{j\eta}$ function as a binary indicator to decide whether the allocated subset of tasks contains elements from I_η .

The set indicator model is NP-hard. We can simply reduce a bin packing problem to this model. Firstly, consider an arbitrary bin packing problem with items $i \in I$ of weight w_i and identical bins of capacity Q . The bin packing problem can be expressed as a decision problem: whether there exists a way to fit items

into $|J|$ bins. This decision problem can be directly mapped onto the set indicator model with an arbitrary nonempty H and $\beta_\eta = 1$ for all $\eta \in H$. Finally, the answer to this decision problem is true if and only if the model provides a feasible solution.

The objective function of the surrogate model can also be presented as a function with y being input. The surrogate model is always feasible for any $y \in P$. Therefore, by assigning a specific value to y , denoted as \hat{y} , we represent the objective value of the surrogate model as:

$$\mathcal{L}_{\beta,H}(\hat{y}) = \min\left\{\sum_{\eta \in H} \beta_\eta \left(\sum_{j \in J} \delta_{j\eta}\right) : y = \hat{y}, (9b), (9c), (9d), (9e), (9f), (9g)\right\}, \quad (10)$$

where $\beta = (\beta_\eta)_{\eta \in H}$.

The objective function $\mathcal{L}_{\beta,H}$ can be further reformulated as a linear combination of different g_H . The property enables our learning procedure to acquire the fittest β_η values. We propose the following proposition on this property.

THEOREM 1. *Let I denote a set of tasks and P its resulting polyhedron of feasible integers in (2). Let H denote a set of indices of $\mathcal{P}^*(I)$ and $\mathcal{L}_{\beta,H}(y)$ a function defined by equation (10) with $\beta_\eta \geq 0$ for all $\eta \in H$. Then*

$$\mathcal{L}_{\beta,H}(y) = \sum_{\eta \in H} \beta_\eta g_{\{I_\eta\}}(s(y)) \quad (11)$$

holds for any $y \in P$.

Proof. For any $y \in P$, we denote J_η for $\eta \in H$ as a subset of J such that $s(y)^k \cap I_\eta \neq \emptyset$ for any $k \in J_\eta$. Therefore, by the definition of g_H , we have $g_{\{I_\eta\}} = |J_\eta|$. Further, under the premise of minimizing $\sum_{\eta \in H} \beta_\eta (\sum_{j \in J} \delta_{j\eta})$, $\delta_{j\eta}^* = 1$ for $j \in J_\eta$ and 0 otherwise. Thus, $\sum_{j \in J} \delta_{j\eta}^* = |J_\eta|$. Finally, $\sum_{\eta \in H} \beta_\eta (\sum_{j \in J} \delta_{j\eta}) = \sum_{\eta \in H} \beta_\eta |J_\eta| = \sum_{\eta \in H} \beta_\eta g_{\{I_\eta\}}(s(y))$.

Following theorem 1, we propose the parameterized version of g_H as follows:

$$g_{\beta,H}(s) = \sum_{\eta \in H} \beta_\eta g_{\{I_\eta\}}(s). \quad (12)$$

The parameterized function $g_{\beta,H}$ extends the problem **(P1)**, incorporating a stronger learning capability by assigning different weights to subsets corresponding to indices within H . Moreover, under the assumption that $\beta \geq \mathbf{0}$, $g_{\beta,H}(s(y)) = \mathcal{L}_{\beta,H}(y)$.

3.2. Learning method

In this subsection, we illustrate the learning method as a process to acquire the parameters β and H of the surrogate model. We first introduce sampling and regression algorithms to acquire β with pre-defined H . Subsequently, we present an iterative training procedure to find H and control model size.

3.2.1. Sampling and regression algorithms We illustrate the sampling method in Algorithm 1. The algorithm randomly selects a feasible point within the polyhedron P in equation (2). This selection is achieved by setting a random assignment cost c as the objective function. Given that every integer point in P is an extreme point, the algorithm guarantees that every solution has a non-zero probability of being selected. Algorithm 1 can be executed in parallel N times to construct a training dataset. Assuming we have gathered $s(y_i)$ and $f_{\text{obj}}(y_i)$ for $i = 1, 2, \dots, N$, we denote the collection of all assignment plans as S_N and the corresponding objective values as b_N .

Algorithm 1 Monte-Carlo sampling

Require: Task set I , agent set J , weights of each task w_i for $i \in I$, and agent capacity Q

- 1: Formulate polyhedron P by (2) into a MIP solver
 - 2: Generate random $c_{ij} \in [0, 1]$ for $i \in I$ and $j \in J$
 - 3: Solve $\min_{y \in P} \sum_{i \in I} \sum_{j \in J} c_{ij} y_{ij}$ by the MIP solver with optimal solution as \hat{y}
 - 4: Storage $s(\hat{y})$ and $f_{\text{obj}}(\hat{y})$
-

By theorem 1, $\mathcal{L}_{\beta, H}$ can be presented as a weighted linear combination formulation, with different g_H being predictors. This formulation allows linear regression methods on the collected data. Therefore, to implement a regression process with a pre-defined set H , we initially construct the feature matrix. Let $A(S_N, H)$ represent a matrix with N rows and $|H|$ columns. Denote the j -th element in H as h_j . The entry in the matrix $A(S_N, H)$ located at the i -th row and j -th column is indicated as $A(S_N, H)_{ij}$ as

$$A(S_N, H)_{ij} = g_{\{h_j\}}(s(y_i)). \quad (13)$$

Let $\mathbb{N}_{|\mathcal{P}^*(I)|}$ be $\{1, 2, \dots, |\mathcal{P}^*(I)|\}$. As a set of indices, H is a subset of $\mathbb{N}_{|\mathcal{P}^*(I)|}$. Therefore, $A(S_N, H)$ is a submatrix of $A(S_N, \mathbb{N}_{|\mathcal{P}^*(I)|})$ for any S_N . Below, we present a specific example for illustration.

EXAMPLE 1. Consider a GAPR instance with a set of items $I = \{1, 2, 3\}$ and a set of agents $J = \{1, 2\}$. An assignment plan s can be presented as an ordered 2-partition of the set I . Suppose we sampled three specific assignment plans, namely s_1 , s_2 , and s_3 . The matrix $A(S_N, \mathbb{N}_{|\mathcal{P}^*(I)|})$ can be delineated in Table 1. Furthermore, if we set $H = \{4, 5, 6\}$ as the indices corresponding to $\mathcal{P}^*(I)$, then the matrix $A(S_N, H)$ can be presented as the blue-colored submatrix within Table 1.

Table 1 The matrix $A(S_N, \mathbb{N}_{|\mathcal{P}^*(I)|})$ for three specific assignment plans, highlighting submatrix $A(S_N, H)$ with $H = \{4, 5, 6\}$ in blue

s	{1}	{2}	{3}	{1,2}	{1,3}	{2,3}	{1,2,3}
$s_1 = (\{1\}, \{2, 3\})$	1	1	1	2	2	1	2
$s_2 = (\{2\}, \{1, 3\})$	1	1	1	2	1	2	2
$s_3 = (\{3\}, \{1, 2\})$	1	1	1	1	2	2	2

Let b_N be the vector of collected objective values. Following theorem 1, the regression problem can be expressed as a non-negative least-square as follows:

$$\min_{\beta \geq \mathbf{0}} \|A(S_N, H)\beta - b_N\|_2. \quad (14)$$

However, in the implementation phase, we adopt a lasso regression model as follows:

$$\min_{\beta} \|A(S_N, H)\beta - b_N\|_2 + \gamma \|\beta\|_2 \quad (15)$$

The additional regularization term controls our model size. We also drop non-negative constraints on the regression coefficients β for speedy computing. Moreover, the resultant negative value of certain β_η merely results in the objective value of the related $\sum_{j \in J} \delta_{j\eta}$ into a constant, without influencing the optimization outcome of the surrogate model.

3.2.2. Training and solving procedure We design the training and solving process as an iterative procedure. A primary consideration here is that the set of H has an exponentially large number of possibilities, rendering it impractical to incorporate all possibilities simultaneously in the regression process. Additionally, it is crucial to ensure that the surrogate model remains of a small size, considering the efficiency of optimization.

We summarize the training procedure in Algorithm 2. We utilize a greedy search strategy to explore the set H . The search starts from a predetermined cardinality π_{card} . Consider indices of all subsets in $\mathcal{P}^*(I)$ with the cardinality of π_{card} as potential candidates for H . Subsequently, a parameter θ is introduced to control the scale of the regression model in equation(15), ensuring that the size of H does not exceed θN . If H is within the threshold of θN , all candidate indices are included in the current H . If it exceeds, only the top θN candidate indices are considered. The process progresses by increasing the π_{card} by one if all candidate indices have been explored.

Following the determination of H in each iteration, we compute the feature matrix $A(S_N, H)$ and the regularization coefficient γ . The regression model (15) is solved as an optimization problem. To evaluate the current model's quality, we compute the R-squared value. If satisfactory, we include the obtained optimal β^* to model (9), yielding an assignment solution y^* by optimizing. Subsequently, the objective value corresponding to y^* is computed as z . The next process involves assessing whether this objective value is the best so far; if so, the search continues, otherwise, the program terminates.

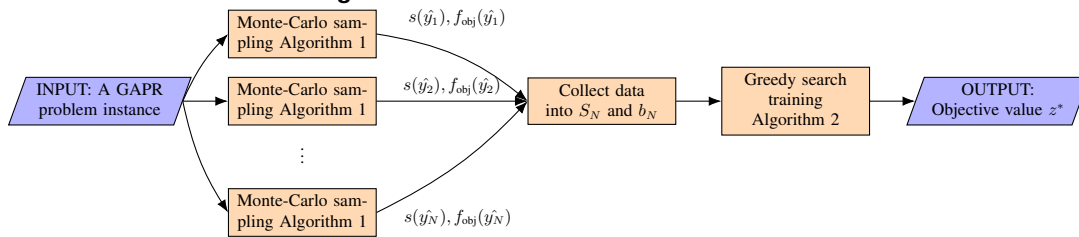
Algorithm 2 Greedy search training**Require:** $\theta, \pi_{card}, \pi_{limit}, \gamma(A, b), S_N, b_N$;

- 1: Initialize $z^* \leftarrow \infty, H \leftarrow \emptyset, \bar{H} \leftarrow \emptyset$;
- 2: **while** $\pi_{card} \leq \pi_{limit}$ **do**
- 3: **if** $\bar{H} = \emptyset$ **then**
- 4: $\bar{H} \leftarrow$ indices of all subsets in $\mathcal{P}^*(I)$ with cardinality of π_{card} ;
- 5: $\pi_{card} \leftarrow \pi_{card} + 1$;
- 6: **end if**
- 7: **if** $|H| + |\bar{H}| \leq \theta N$ **then**
- 8: $H \leftarrow H \cup \bar{H}$;
- 9: $\bar{H} \leftarrow \emptyset$;
- 10: **else**
- 11: $\{\bar{h}_1, \bar{h}_2, \dots\} \leftarrow \bar{H}$;
- 12: $H \leftarrow H \cup \{\bar{h}_1, \bar{h}_2, \dots, \bar{h}_{\lfloor \theta N \rfloor - |H|}\}$;
- 13: $\bar{H} \leftarrow \{\bar{h}_{\lfloor \theta N \rfloor - |H|}, \dots\}$;
- 14: **end if**
- 15: $\gamma \leftarrow \gamma(A(S_N, H), b_N)$;
- 16: Solve regression problem (15) and obtain optimal solution β^* ;
- 17: Compute the R-squared value on the regression result as R^2
- 18: $H \leftarrow \{\eta : \beta_\eta^* \neq 0\}$;
- 19: $\beta^* \leftarrow (\beta_\eta)_{\eta \in H}$;
- 20: **if** $R^2 > R_{limit}$ **then**
- 21: Solve surrogate model (9) built by parameters β^* and H . Obtain optimal solution y^* ;
- 22: $z \leftarrow f_{obj}(y^*)$;
- 23: **if** $z^* > z$ **then**
- 24: $z^* \leftarrow z$;
- 25: **else**
- 26: **break**;
- 27: **end if**
- 28: **end if**
- 29: **end while**

Finally, we present the workflow of our method in Figure 2. Given a GAPR instance, we run N sampling algorithms in parallel to obtain a data set S_N and b_N . We then feed the data into Algorithm 2 for iterative

training. Then we obtain the final objective function value z^* . Concurrently, the optimal values of decision variables y and u in the model (1) for practical planning can also be derived by computing the objective value.

Figure 2 The flow chart of learning method



4. Theoretical analysis

This section theoretically explores the effectiveness of our framework. We first examine its representational power, which is a property closely associated with learning capacity. We further provide statistical estimation results to validate the effectiveness of our surrogate models to produce solutions as an approximation to the original formulations

4.1. Representational power

Our model utilizes a finite set of features as predictors, raising questions regarding its learning capacity. The central inquiry pertains to the model's ability to accurately fit varying objective functions specific to the GAPR problems. This concept has been discussed in studies of neural networks, particularly for graph neural networks (GNN) (Azizian and Lelarge 2021). The study by Chen et al. (2022) further extended this discussion into learning the objective values of general MIP by GNN while delineating representational power into two fundamental aspects: separation power and approximation power. Subsequently, we follow the scheme of Chen et al. (2022) by providing theoretical results on our method.

The separation power can be initially stated as follows: an equivalence relation between two inputs exists if, and only if, any given function produces identical outputs for these inputs. For the GAPR, we first define the equivalent relationship as follows.

DEFINITION 2. Two solutions $y_1, y_2 \in P$ are equivalent if there exists a permutation ϕ such that $s(y_1) = \phi(s(y_2))$.

Then we show that our surrogate model has separation power by the following theorem.

THEOREM 2. Two solutions $y_1, y_2 \in P$ are equivalent if and only if $\mathcal{L}_{\beta, H}(y_1) = \mathcal{L}_{\beta, H}(y_2)$ for any β and H .

Proof. We use the condition of equivalent and its converse to prove the necessary and sufficient conditions.

(1). If y_1 and y_2 are equivalent, then for any β and H , denote $\delta_{j\eta}^{(1)}$ and $\delta_{j\eta}^{(2)}$ as the optimal solution of model (9) with fixing y to y_1 and y_2 . If β_η is non-negative, then

$$\sum_{j \in J} \delta_{j\eta}^{(1)} = g_{\{I_\eta\}}(s(y_1)) \quad (16)$$

$$= \sum_{j \in J} \mathbf{1}_{I_\eta \cap s(y_1)^j \neq \emptyset} \quad (17)$$

$$= g_{\{I_\eta\}}(\phi(s(y_1))) \quad (18)$$

$$= \sum_{j \in J} \delta_{j\eta}^{(2)}. \quad (19)$$

If β_η is negative, then $\sum_{j \in J} \delta_{j\eta}^{(1)} = \sum_{j \in J} \delta_{j\eta}^{(2)} = |J|$. Finally, we obtain that $\mathcal{L}_{\beta,H}(y_1) = \mathcal{L}_{\beta,H}(y_2)$ for any β and H .

(2). Conversely, assume y_1 and y_2 are not equivalent. we set $\beta_\eta = 1$ for any η . This ensures that for any feasible input y , $\mathcal{L}_{\beta,H}(y) = g_H(s(y))$, where $s(y)$ denote the corresponding assignment plan s for y . We define $s_1 = s(y_1)$ and $s_2 = s(y_2)$ for simplicity.

We can propose that there exist an index k_1 such that $s_1^{k_1} \neq s_2^{k_2}$ for all $k_2 \in J$. To contradict this assertion is to suggest that for every $k_1 \in J$, there exists a corresponding k_2 such that $s_1^{k_1} = s_2^{k_2}$. Such a scenario implies that s_1 and s_2 are merely different permutations of identical subsets of I . However, this would imply $f(y_1) = f(y_2)$ under the assumption of homogeneity among agents, contradicting our initial condition. Given the existence of such a k_1 , we consider two scenarios.

Firstly, if there exists a k_2 such that $s_1^{k_1}$ is a subset of $s_2^{k_2}$, we define $H = \{\eta : I_\eta = s_2^{k_2}\}$. In this scenario, elements of $s_2^{k_2}$ are found in more than one subset within s_1 , leading to $\mathcal{L}_{\beta,H}(y_2) = 1 < \mathcal{L}_{\beta,H}(y_1)$.

Conversely, $s_1^{k_1}$ does not form a subset of any subset in s_2 , implying its elements are distributed across multiple subsets in s_2 . we define $H = \{\eta : I_\eta = s_1^{k_1}\}$. Thus, $\mathcal{L}_{\beta,H}(y_1) = 1 < \mathcal{L}_{\beta,H}(y_2)$.

Therefore, there exist some $\mathcal{L}_{\beta,H}(y_1)$ that output differently.

Upon proving the separation power, we can further show that in the best scenario, our surrogate model is able to identify a solution that is either identical to or equivalent to that derived from the original model.

COROLLARY 1. *Let (y^*, u^*) denote the optimal solution to a given instance of GAPR defined by model 1. There exists a surrogate model represented by $\mathcal{L}_{\beta,H}$ such that the equation $y = \arg \min_y \mathcal{L}_{\beta,H}(y)$ holds if and only if y is equivalent to y^* .*

Proof. Let $s^* = s(y^*)$. Set $H = \{\eta \mid \exists k \in J \text{ such that } I_\eta = s^{*k}\}$ and $\beta = \mathbf{1}$. According to Theorem 1, $\mathcal{L}_{\beta,H}(y) = g_{\beta,H}(s(y)) = \sum_{\eta \in H} g_\eta(s(y))$. Here, $g_\eta(s(y)) = \sum_{k \in J} \mathbf{1}_{I_\eta \cap s(y)^k \neq \emptyset} \geq 1$, leading to $\mathcal{L}_{\beta,H} \geq |H|$. It can be computed that $\mathcal{L}_{\beta,H}(y^*) = g_{\beta,H}(s^*) = |H|$. Thus y^* is the minimal solution of $\mathcal{L}_{\beta,H}$.

Further, by Theorem 2, any y which is equivalent to y^* also minimizes $\mathcal{L}_{\beta,H}$. Conversely, if y is not equivalent to y^* , it implies a discrepancy of elements in sequences $s(y)$ and $s(y^*)$. This discrepancy guarantees the presence of some η for which $g_\eta(s(y)) \geq 2$, thereby disqualifying y as the minimal solution of $\mathcal{L}_{\beta,H}$. This completes the proof.

The approximation power involves the error between the surrogate model and the learning target. We provide an upper bound on the training error of equation (15) for any pre-defined H without the regulation term. This result generally applied to all GAPR problems.

THEOREM 3. *Given a set of tasks I and a set of agents J , with an overdetermined matrix $A(S_N, H)$, and the normalized $\bar{b}_N = \frac{b_N}{\|b_N\|}$. Let $A = A(S_N, \mathbb{N}_{|\mathcal{P}^*(I)|})$ and λ_{max} denote the largest eigenvalue of $\mathbf{Id} - A(A^\top A)^{-1}A^\top$, where \mathbf{Id} is the unit matrix. It follows that*

$$\min_{\beta \in \mathbb{R}^{|\mathcal{H}|}, H \subseteq \mathcal{P}^*(I)} \|A(S_N, H)\beta - \bar{b}_N\| \leq \sqrt{\lambda_{max}}$$

Proof. We begin by noting, as illustrated in Example 1, that the matrix $A(S_N, H)$ is a submatrix of A . The selection of columns from A to form $A(S_N, H)$ can also be controlled by the vector β by setting certain values to be zeros. Thus, we have

$$\min_{\beta \in \mathbb{R}^{|\mathcal{H}|}, H \subseteq \mathcal{P}^*(I)} \|A(S_N, H)\beta - \bar{b}_N\| = \min_{\beta \in \mathbb{R}^{|\mathcal{P}^*(I)|}} \|A\beta - \bar{b}_N\|. \quad (20)$$

The optimal solution to this least squares problem is given by $\beta^* = (A^\top A)^{-1}A^\top \bar{b}_N$.

Proceeding, we find that

$$\begin{aligned} \|A\beta^* - \bar{b}_N\|^2 &= \bar{b}_N^\top \bar{b}_N - 2\bar{b}_N^\top A\beta^* + (A\beta^*)^\top (A\beta^*) \\ &= \bar{b}_N^\top (\mathbf{Id} - A(A^\top A)^{-1}A^\top) \bar{b}_N. \end{aligned}$$

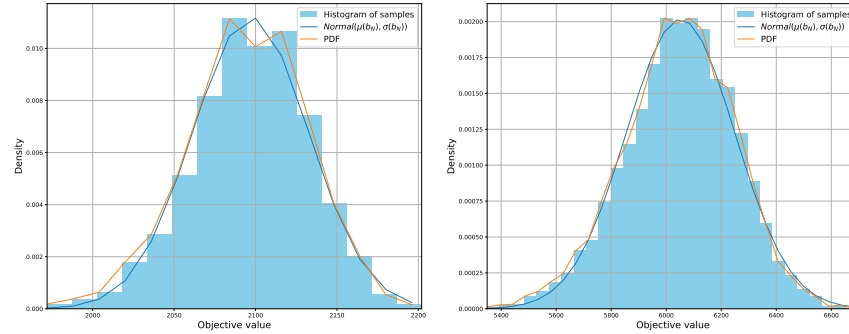
We denote $\mathbf{Id} - A(A^\top A)^{-1}A^\top$ by W . Thus, $\|A\beta^* - \bar{b}_N\|^2 = \bar{b}_N^\top W \bar{b}_N$. Given that $\bar{b}_N^\top W \bar{b}_N \geq 0$ for any \bar{b}_N , it follows that W is positive semidefinite. Furthermore, as $A(A^\top A)^{-1}A^\top$ is symmetric, W is also symmetric. We have $W = U\Lambda U^\top$, where U is an orthogonal matrix and Λ is a diagonal matrix with the eigenvalues of W on its diagonal. For any $\bar{b}_N \in \mathbb{R}^N$ with $\|\bar{b}_N\| = 1$, we have $\bar{b}_N^\top W \bar{b}_N = \bar{b}_N^\top U\Lambda U^\top \bar{b}_N$. Setting $z = U^\top \bar{b}_N$ yields $\|z\| = 1$ and $\bar{b}_N^\top W \bar{b}_N = z^\top \Lambda z \leq \lambda_{max} \|z\| = \lambda_{max}$, with λ_{max} being the largest eigenvalue on the diagonal of Λ . Therefore, we conclude that

$$\|A\beta^* - \bar{b}_N\| \leq \sqrt{\lambda_{max}}.$$

Together with equation (20), we have the theorem result.

4.2. Statistical analysis

We further propose theoretical results for estimating the objective value that our surrogate model yields. The key idea is to use statistical tools to analyze the collected samples. Given that the surrogate model is built from data, it is challenging to derive a general approximation ratio analysis as to the traditional

Figure 3 Solution distribution of the GAPR problems introduced in Section 5

(a) Joint order batching and picker routing problem (b) soft-clustered vehicle routing problem

approximation algorithms. However, it remains possible to estimate the objective value based on statistical inference and the optimization results of the surrogate model.

The utilization of statistical tools involves a new perspective: considering the objective value of an MIP formulation as a random variable. Despite that the feasible solutions for an MIP are usually finite, their massive amount allows the investigation of statistical properties, including statistical distribution. The exploration of statistical properties of solutions to optimization problems has been discussed in many studies. For GAP, a study by Maniezzo et al. (2021) noted that on a small GAP instance, the distribution representing the objective values of all possible solutions can be fitted by a binomial distribution. For the GAPR, we consider the predefined assignment plan s as an event. If an event s happens, the value of the random variable is given by a specific objective function $f(y(s))$, such as the function f_{obj} in equation (3). The detailed definition is as follows.

DEFINITION 3. Let $(\Omega, \mathcal{F}, \mathbb{P})$ be a probability space, where the sample space Ω is the set of all feasible assignment plans s , the event space \mathcal{F} is the power set of Ω , and $\mathbb{P}(s)$ is the probability for s to be sampled. Denote the objective function as f . Define random variable $X^f(s)$ as mapping

$$s \mapsto f(y(s)),$$

where f is a real-valued function.

We first infer the distribution of random variables based on the objective function. To simplify notations, we denote the random variable defined by the objective function (3) as X^f , and that defined by the function $g_{\beta, H}$ as Y^g . Experiments are conducted on two distinct classes of the GAPR problems that are described in detail in Section 5. From each instance, a collection of 6,000 samples of objective values is sampled. These samples are subsequently represented in bar charts, alongside the empirical probability density function (PDF) to closely approximate their true distribution curve. Two typical plots are exhibited in Figure 3. Moreover, we conduct Chi-squared tests to check whether or not the PDFs follow the normal distribution. The results all indicate that the samples can be fitted by normal distributions.

The distribution tests provide strong support to the assumption the distributions of X^f and Y^g can be approximated by the normal distribution for subsequent estimations. Under this premise, We consider the scenario upon training a surrogate model in the form of model (9) and solving it to a solution denoted as \hat{y} , yielding $\hat{Y} = g_{\beta,H}(s(\hat{y}))$. Therefore, We can estimate the expected value of the true value of $f_{\text{obj}}(\hat{y})$, without computing an optimization problem. We consider the subsequent theorem.

THEOREM 4. *Let X^f and Y^g be random variables defined by the definition 3. If (X^f, Y^g) follow bivariate normal distribution, then*

$$(X^f, Y^g) \sim \text{Normal} \left((\mu_X, \mu_Y), \begin{bmatrix} \sigma_X^2 & \rho\sigma_X\sigma_Y \\ \rho\sigma_X\sigma_Y & \sigma_Y^2 \end{bmatrix} \right). \quad (21)$$

Given $Y^g = \hat{Y}$, the conditional expectation of X^f is

$$\mathbb{E}[X^f | Y^g = \hat{Y}] = \mu_X + \sigma_X \rho \frac{\hat{Y} - \mu_Y}{\sigma_Y}. \quad (22)$$

The upper bound ζ that $P(X^f < \zeta | Y^g = \hat{Y}) = 1 - \alpha$ is

$$\zeta = \sigma_{X|Y} \Phi^{-1}(1 - \alpha) + \mu_{X|Y}, \quad (23)$$

where $\mu_{X|Y} = \mu_X + \sigma_X \rho \frac{\hat{Y} - \mu_Y}{\sigma_Y}$, $\sigma_{X|Y} = (1 - \rho^2) \sigma_X$ and $\Phi(\zeta) = \frac{1}{\sqrt{2\pi}} \int_{-\infty}^{\zeta} e^{-t^2/2} dt$.

Proof. The statistical properties utilized in this theorem can be found in multivariate statistical analysis (Härdle et al. 2007). By the assumption of bivariate normal distribution, the conditional probability density function of X^f is

$$f_{X|Y}(X^f) = \frac{f_{Y,X}(Y^g, X^f)}{f_Y(Y^g)},$$

where

$$f_{Y,X}(Y^g, X^f) = \frac{1}{2\pi\sigma_Y\sigma_X\sqrt{1-\rho}} \exp \left(-\frac{\left(\frac{(Y^g - \mu_Y)^2}{\sigma_Y^2} + \frac{(X^f - \mu_X)^2}{\sigma_X^2} - \frac{2\rho(Y^g - \mu_Y)(X^f - \mu_X)}{\sigma_Y\sigma_X} \right)}{2(1-\rho^2)} \right),$$

and

$$f_Y(Y^g) = \frac{1}{\sqrt{2\pi}\sigma_Y} \exp \left(-\frac{(Y^g - \mu_Y)^2}{2\sigma_Y^2} \right).$$

Therefore, the conditional distribution follows

$$X^f | Y^g = \hat{Y} \sim \text{Normal} \left(\mu_X + \rho \frac{\sigma_Y}{\sigma_X} (\hat{Y} - \mu_Y), (1 - \rho^2) \sigma_X^2 \right).$$

This distribution directly shows the expected value of X^f . Moreover, based on the upper bound as

$$P(X^f < \zeta | Y^g = \hat{Y}) = 1 - \alpha,$$

we have

$$\Phi\left(\frac{\zeta - \mu_{X|Y}}{\sigma_{X|Y}}\right) = 1 - \alpha.$$

Then, with the known upper critical value we have the result

$$\zeta = \sigma_{X|Y} \Phi^{-1}(1 - \alpha) + \mu_{X|Y}.$$

Assume our regression process yields a statistically significant correlation coefficient ρ . The obtained value \hat{Y} , as a minimized objective value in the surrogate model (9), diverges from its average μ_Y . Consequently, by equation (22)-(23), the value of X^f can be expected to diverge downwards from its average μ_X , indicating a potentially high-quality solution.

5. Numerical experiments

In this section, we examine our methodology through numerical experiments conducted on two distinct GAPR problems. We address the following experimental questions. **Q1)** How accurately do our proposed surrogate models approximate solutions when compared to exact models? **Q2)** Do our surrogate models significantly enhance solving efficiency? Given that our surrogate models are NP-hard, it is important to empirically verify the improvement in computational efficiency. **Q3)** Can the observed improvements be attributed to the modifications introduced in the MIP formulations? This question investigates the causality behind improvements to further enhance the understanding of the contribution of our methodology. The notations for data presentation are listed in Table 2.

Finally, to further demonstrate the practical efficiency of our approach, we compare our algorithm with the best-known heuristics. Notably, these state-of-the-art heuristics hold a priori knowledge of specific problems to tailor their strategies, thereby exploiting the inherent characteristics of these problems to improve efficiency. In contrast, our generalized approach increases the challenge by omitting the prior knowledge and problem features. However, this approach offers the advantage of adaptability, eliminating the need to redesign in the context of new problems.

For the experiments, we employ GUROBI version 9.5.1 as a branch-and-cut (B&C) solver, operating in a black-box way without customized algorithmic configurations. We set the sample size N to 6000 and the parameters $\pi_{card} = 3$, $\pi_{limit} = 5$, and $R_{limit} = 0.5$ in Algorithm 2. The parameter θ in Algorithm 2 is set to 0.2 in Section 5.1, and in Section 5.2, it is 0.2 if $|J| < 40$ and 0.5 otherwise. The parameter θ in Algorithm 2 is set to 0.2 in 5.1 and The setting of the regulation parameter in the regression follows Zou et al. (2007). Experiments are implemented in the Python language. We use a workstation of Intel Xeon E5-2699 v4 2.20 gigahertz CPU for sampling and a personal computer (Intel i7 2.60 gigahertz CPU, 16-gigabyte memory) with Windows 10.0. for comparison tests. Additionally, to facilitate a clear and structured presentation of our comparative analysis, we introduce specific notations in Table 2. These notations are designed to display the relative performance and efficiency data between the tested models.

Table 2 Parameters for instance generation

Notation	Description
SIM	The set indicator model
Exact	The exact model for comparison
Δ	Instance group identifier
Nodes	Number of explored nodes within the B&C procedure
Rows	Number of constraints of a MIP before presolving
Cols	Number of variables of a MIP before presolving
Obj	Objective value (computed by equation (3) for SIM)
Time _{MIP}	CPU computing time in seconds of solving MIP models of SIM or Exact
Time _{Total}	Total CPU computing time in seconds, including the average time to conduct Algorithm 1 once and the time for Algorithm 2.
Gap	Integrality gap
Alg1 / Alg2	Objective ratio of algorithms denoted by Alg1 and Alg2.
Min(sample)	Minimal objective value of samples

5.1. Case study I: the joint order batching and picker routing problem (JOBPRP)

We adopt the problem setting of Valle et al. (2017) to JOBPRP with a warehouse configuration that comprises multiple identical vertical storage racks, separated by navigable aisles. Each rack is divided into several blocks, with each block storing a specific type of item. Orders are composed of one or more items, and items belonging to the same order must be grouped into a single batch. The process of handling a batch involves a picker departing from a depot, traversing through the blocks for picking, and subsequently returning to the depot. The distance between any two blocks is calculated using the Manhattan distance metric.

The JOBPRP has attracted significant academic interest in the field of warehouse management studies, as highlighted in the comprehensive review conducted by Van Gils et al. (2018). The JOBPRP is initially proposed by Won and Olafsson* (2005). For exact B&C algorithms, the work by Valle et al. (2016) presented three basic formulations. Two of them are based on network flows, with the remaining one having exponentially increasing constraints. Furthermore, real-world data sets were included in the study of this problem (Valle et al. 2016). In a subsequent advancement, the work by Valle et al. (2017) enhanced these formulations with valid inequalities. The study by Zhang and Gao (2023) further made significant improvements by reformulating the connectivity constraints within the JOBPRP. Additionally, several heuristics and meta-heuristics have also been proposed for this problem in the past decade Cheng et al. (2015), Lin et al. (2016), Li et al. (2017), Valle and Beasley (2020).

In this study, we compare with the latest study of the exact approach by Zhang and Gao (2023). Compared with Valle et al. (2017), the new formulation by Zhang and Gao (2023) increases the number of optimally solved instances within 2400 seconds by 50%. In scenarios involving over ten orders where both algorithms achieve optimal solutions, the new formulation ensures a minimum of 54% reduction in solution time. We adopt the same benchmark instances as Valle et al. (2017), Zhang and Gao (2023).

5.1.1. Experiment results Table 3 presents detailed information and solutions on 39 instances from the SIM and Exact model. On average, the distance in objective values between SIM and the Exact is within 1%. The SIM performs equal or better in one-third of all the instances. On average, SIM reduces the solution time by 95%, demonstrating a significant total time advantage. These results strongly indicate the precision and efficiency of the SIM, as answers to questions **Q1** and **Q2**.

We visualize part of the data for further analysis. Figure 4 depicts a scatter plot of the number of constraints versus the number of variables for both the SIM and the Exact across different instances, with the number of constraints on the x-axis and the number of variables on the y-axis. It is observable that the distribution of the SIM is relatively concentrated within the range of 80-2000. In contrast, the distribution of data for the Exact shows an incremental trend with the increase in the scale of instances. This demonstrates that our framework is capable of stably generating MIP models of far less scale.

Figure 5 presents a bar graph illustrating the average explored nodes during the B&C process for different amounts of orders. For the Exact, the node number increases rapidly before 22 orders, caused by the rapid growth of model size. Beyond 22 orders, due to the time limit and model complexity, the B&C process stops early, leaving a sharp decline followed by a gradual decrease in the figure. Conversely, for the SIM, the nodes remain at a lower level with a slow growth trend. This aligns with the SIM's limited number of variables in Figure 4.

In Figure 6, we visualize the collected data for the instances of Day20 with 40 orders, as a typical example. The scatter plot presents the Exact objective values on the x-axis and the learned approximate function g values on the y-axis. This plot exhibits a bivariate normal distribution. The formula (22) from Theorem 4 is represented as a straight line through statistical estimations. It is observed that the solution by the SIM is situated close to its expected value and is significantly lower than all sampled values. In Figure 7, we further illustrate the average SIM objective values for different amounts of orders alongside the minimum sampled objective values. The objective values from the SIM are increasingly lower than that of the sampled values. This evidence indicates that our framework outperforms mere Monte Carlo sampling, being able to learn optimization models to discover new solutions.

The remarkable improvements demonstrated by the SIM can be attributed to our modifications of the MIP formulations, specifically, the replacement of routing constraints with big-M constraints. Thus the question **Q3** is answered. Firstly, considering that the experiment setting utilizes the same solving procedure, the only varying factor is the formulation structure. Moreover, the empirical evidence shown in Figure 4 and 5 indicates that our framework consistently generates MIP models of smaller size, alongside reductions in the B&B tree sizes. These outcomes corroborate the efficiency shown in the experiment and further prove our motivation expressed in the introduction. Finally, the significant difference in Figure 7 between the SIM and samples demonstrates that our framework does have the ability to find optimization direction and find new solutions.

Additionally, we compare our approach against the best-known heuristic for JOBPRP. We imposed a 20-second time restriction on each surrogate model within Algorithm 2, recognizing that the solution at this limit could represent the optimal outcome. Valle and Beasley (2020) designates this best-known heuristic as PIO, reporting its superior performance over traditional heuristics in effectiveness and efficiency. We utilized the same problem scales as Valle and Beasley (2020). The comparative results are presented in Table 4. The results indicate that our algorithm consistently performs better on small and medium scales. On average, our approach demonstrates better outcomes and reduced computational time.

Table 3 Results for the JOBPRP instances

Instance			SIM						Exact						Exact/SIM	Min(sample)
Δ	Order	Trolley	Obj	Nodes	Rows	Cols	Time _{MIP}	Time _{Total}	Obj	Nodes	Rows	Cols	Gap(%)	Time _{MIP}		
Day5	10	2	582	145	290	288	0.2	18	578	3040	9582	4568	0.00	10	0.99	578
	12	2	630	332	596	594	0.8	14	616	4696	9742	4652	0.00	73	0.98	616
	15	2	652	1	544	542	0.4	23	650	3953	9992	4786	0.00	52	1.00	650
	17	3	832	4316	682	678	5.9	61	802	15481	15244	7317	0.00	271	0.96	864
	20	3	880	221	364	360	0.3	24	864	50341	15529	7446	0.00	917	0.98	886
	22	3	892	2497	1006	1002	9.5	130	892	107936	15724	7536	0.00	1923	1.00	946
	25	4	1120	7266	999	992	13.4	83	1108	25543	21427	10284	25.72	2400	0.99	1190
	27	4	1180	4367	891	884	15.1	90	1154	25575	21651	10388	25.74	2400	0.98	1248
	30	4	1242	4539	695	688	6.0	37	1228	25762	21927	10496	29.64	2400	0.99	1292
	32	5	1358	3575	1046	1035	5.8	26	1346	24390	27591	13170	38.48	2400	0.99	1504
	35	5	1464	3929	1171	1160	14.5	43	1448	13681	28061	13405	42.33	2400	0.99	1548
	37	5	1538	4750	846	835	6.4	39	1506	15362	28316	13515	41.50	2400	0.98	1624
40	6	1712	15454	1924	1908	67.9	183	1642	8612	34336	16332	49.90	2400	0.96	1848	
Day10	10	2	656	1	82	80	0.1	9	656	7598	9988	4768	0.00	34	1.00	656
	12	2	702	1	490	488	0.5	13	702	2501	10212	4884	0.00	40	1.00	702
	15	3	894	4326	862	858	5.6	24	874	39134	15727	7515	0.00	315	0.98	888
	17	3	968	1072	487	483	0.9	16	960	76979	16000	7653	0.00	703	0.99	968
	20	3	1010	372	373	369	0.2	14	984	104755	16267	7758	0.00	1523	0.97	1026
	22	3	1022	762	403	399	0.4	16	1000	66779	16462	7848	0.00	1109	0.98	1032
	25	4	1236	18756	1603	1596	91.9	225	1196	25603	22311	10620	26.84	2400	0.97	1294
	27	4	1274	6731	963	956	6.4	28	1274	25219	22531	10708	26.50	2400	1.00	1350
	30	4	1304	1184	903	896	4.2	45	1286	25145	22851	10832	31.25	2400	0.99	1360
	32	5	1548	4014	1501	1490	32.3	125	1492	20177	28866	13670	37.33	2400	0.96	1628
	35	5	1584	4011	1016	1005	8.1	35	1558	19281	29216	13785	40.44	2400	0.98	1642
	37	5	1648	361	926	915	1.6	24	1590	15872	29491	13895	39.18	2400	0.96	1706
40	6	1784	3713	1804	1788	45.9	133	1800	6874	35812	16812	55.28	2400	1.01	1972	
Day20	10	3	944	491	232	228	0.3	11	912	10920	15367	7344	0.00	112	0.97	912
	12	3	998	3350	646	642	2.1	17	998	35459	15613	7422	0.00	254	1.00	1002
	15	3	1026	1787	505	501	1.3	17	1022	85837	16078	7623	0.00	532	1.00	1036
	17	4	1250	2929	675	668	4.9	23	1250	67364	21859	10348	5.84	2400	1.00	1278
	20	4	1358	7842	871	864	26.1	90	1348	29741	22479	10616	15.87	2400	0.99	1370
	22	5	1542	8062	1091	1080	41.2	127	1570	25508	28531	13440	25.74	2400	1.02	1596
	25	5	1634	4828	1091	1080	39.5	236	1670	25842	29051	13595	34.43	2400	1.02	1698
	27	5	1688	7221	1066	1055	40.4	159	1700	25824	29456	13745	32.82	2400	1.01	1716
	30	6	1954	8451	1354	1338	22.7	80	1940	13284	36064	16752	47.42	2400	0.99	2000
	32	6	1966	7668	1372	1356	19.7	114	1900	13888	36640	17004	50.85	2400	0.97	2052
	35	6	2002	6482	1474	1458	32.8	95	2030	12516	37174	17118	46.15	2400	1.01	2086
	37	7	2226	4110	1765	1743	34.0	182	2246	5403	43800	20069	57.20	2400	1.01	2364
40	7	2264	3150	1793	1771	47.1	315	2330	5306	44374	20174	59.80	2400	1.03	2438	
Average			4181.2	933.4	924.9	16.8	75.4	28645.7	23367.7	11022.9	1678.6	0.99				

5.2. Case Study II: the soft-clustered vehicle routing problem (SoftCluVRP)

The SoftCluVRP represents a variant of the classical CVRP. In SoftCluVRP, customers are partitioned into distinct clusters, with the restriction that all customers belonging to the same cluster must be served by the same vehicle. This requirement introduces an additional layer of complexity compared to the classical CVRP. Moreover, unlike the hard-clustered variant of this problem, where a vehicle must completely serve

Figure 4 Scatter of model sizes

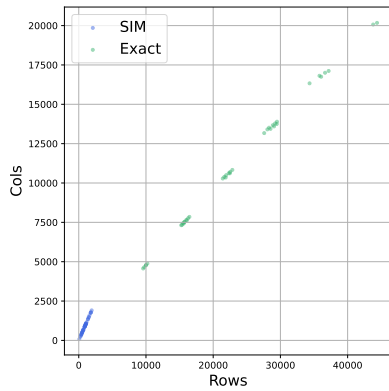


Figure 5 Explored nodes during the B&C process

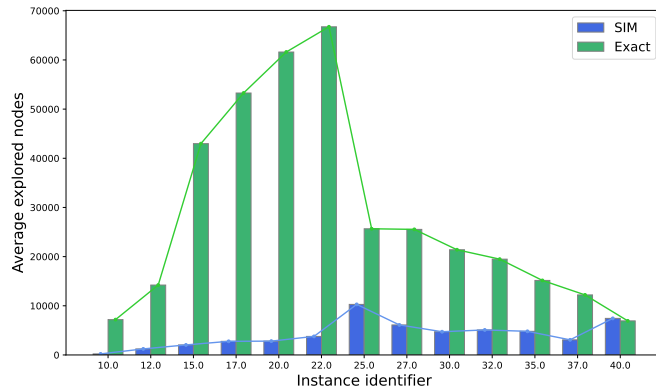


Figure 6 Parity plot of training and prediction of the SIM and Exact models

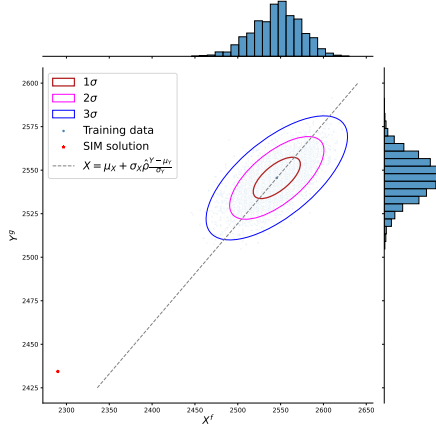


Figure 7 The comparison of average group objective values of the SIM the Min(sample)

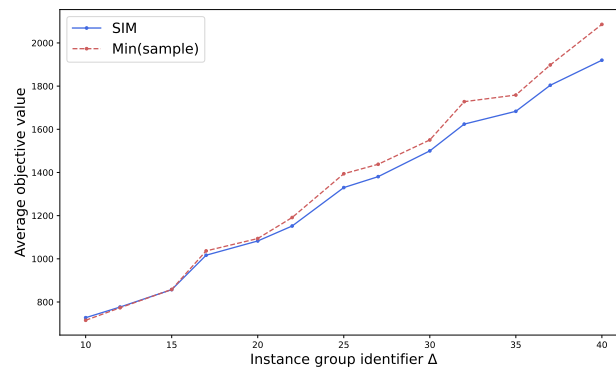


Table 4 The SIM in JOBPRP heuristic comparison

Instance	SIM(20s)		PIO		PIO/SIM		
	Δ	Order	Obj	Time _{Total}			
Day5	25		1120	67	1137.8	1	1.02
	30		1198	167	1267.9	3	1.06
	50		2032	154	2010.5	23	0.99
	75		2974	297	2884.8	648	0.97
Day10	25		1236	34	1251.3	1	1.01
	30		1300	26	1364.9	3	1.05
	50		2174	175	2184.4	29	1.00
	75		3140	776	3125.8	1903	1.00
Day20	25		1630	102	1708.8	2	1.05
	30		1908	149	1954.8	3	1.02
	50		2688	142	2754.6	54	1.02
	75		4006	1120	3849.0	659	0.96
Average				267.4		277.4	1.01

one cluster before proceeding to the next, SoftCluVRP allows for a more flexible approach. In this variant, a vehicle can interrupt service to a cluster to serve customers in another cluster, and then return to the previous cluster if necessary. This flexibility in service sequence allows more efficient routing strategies. However, this flexibility also increases the complexity involved in routing decisions. The problem aims to find an optimal set of routes for a fleet of vehicles that minimizes the total travel cost while ensuring that each cluster's customers are exclusively served by a single vehicle, and adhering to classical CVRP constraints. Moreover, to enhance the diversity of \bar{H} in Algorithm 2 for large instances, we apply a random permutation each time it is newly assigned. As our algorithm becomes non-deterministic in this scenario, we perform 5 experimental rounds per instance, recording the best and average objective values as Obj_{best} and Obj_{avg} , respectively. Additional model data for the SIM is also displayed along with their average values.

The clustered vehicle routing problem was initially introduced by Sevaux and Sörensen (2008) as a practical problem. Subsequently, Defryn and Sörensen (2017) involved soft constraints in customer cluster assignments, implying that such modifications could result in significant cost reduction. Exact methods have been proposed by Hintsch and Irnich (2020). Heuristics have also been proposed by Hintsch (2021). We refer to the review in the study by Hintsch (2021) for a detailed investigation. In this experiment, we adopt the latest B&C algorithm by Heßler and Irnich (2021), which has been examined to be significantly effective. We use the well-known `Golden` benchmark instances (Hintsch and Irnich 2020, Hintsch 2021, Heßler and Irnich 2021). This benchmark encompasses a collection of 220 large-scale instances, with 201 to 484 customers and 14 to 97 clusters. The benchmark is derived from 20 original instances, distinguished by varying clusters, and grouped based on the identifiers of the original instances. Limited by computing resources to conduct Monte-Carlo on large instances, we conduct our comparison on 110 instances with customers no more than 400.

5.2.1. Experiment results Table 5 and 6 present the details and solution outcomes for the SIM and the Exact. To verify the accuracy of our reproduced results, we record the number of instances solved to optimal. Among all considered instances, 35 achieved the optimal solution. This surpasses the original result of 21 by Heßler and Irnich (2021), indicating that our reproduction is not inferior to the original performance. We can measure the effectiveness of the SIM by the win rate, which denotes the proportion of instances in each group where the SIM's results surpassed that of the Exact. Out of 110 cases, SIM's best objective values outperformed the Exact in 64 instances. Moreover, Exact's best objective value is on average 4% larger than that of the SIM. Finally, In comparison to the Exact under a 3600-second time limit, the SIM requires 146.7 seconds of computation time on average, which is only 5% of that of the Exact. These results underscore the significant accuracy and efficiency of SIM in addressing this problem. Thus the questions **Q1** and **Q2** are answered.

Following the analysis approach used in Case I, we show the model details in Figure 8. It is evident from the figure that the model size of the SIM is concentrated within a smaller range of 2000 to 10000, whereas

Table 6 Detailed results for the SoftCluVRP instances (Part2)

Δ	Cluster	Customer	SIM							Exact					Min(sample)	Exact/SIM _{best}		
			Obj _{best}	Obj _{avg}	Nodes	Rows	Cols	Gap(%)	Time _{MIP}	Time _{total}	Obj	Nodes	Rows	Cols			Gap(%)	Time _{MIP}
13	17	253	535	535.0	2014	3353	3396	0.0	2	12	530	51520	32049	32031	0.0	407	548	0.99
13	19	253	530	533.6	5863	3210	3259	0.0	5	36	521	7346	33220	32068	0.0	207	543	0.98
13	20	253	532	532.0	4597	3258	3310	0.0	3	37	521	51999	33820	32088	0.0	489	549	0.98
13	22	253	533	533.8	2319	3409	3467	0.0	4	16	523	50875	35209	32131	0.0	840	558	0.98
13	23	253	533	533.0	3292	3458	3519	0.0	4	24	523	63188	35965	32154	0.0	675	560	0.98
13	26	253	531	532.2	4990	3354	3424	0.0	7	27	523	132609	38705	32229	0.0	1513	579	0.98
13	29	253	534	537.0	6656	3316	3395	0.0	9	28	522	103643	42111	32313	0.0	1584	580	0.98
13	32	253	530	533.2	2363	3603	3691	0.0	4	17	521	84100	46222	32406	0.0	1922	579	0.98
13	37	253	533	537.8	3490	3369	3472	0.0	18	41	551	152979	55002	32581	5.6	3600	593	1.03
13	43	253	533	536.0	3930	9538	9659	0.0	11	84	521	67687	69112	32824	0.0	2790	611	0.98
13	51	253	538	547.0	4103	9463	9608	0.0	24	122	522	41502	95097	33204	0.4	3600	631	0.97
17	17	241	393	393.2	969	2427	2455	0.0	1	9	386	42444	28814	29073	0.0	223	410	0.98
17	18	241	393	393.0	934	2342	2372	0.0	1	8	385	20643	29354	29091	0.0	235	407	0.98
17	19	241	388	388.0	2866	2358	2390	0.0	2	10	385	27296	29962	29110	0.0	305	415	0.99
17	21	241	388	388.0	4108	2360	2396	0.0	5	15	385	38918	31237	29151	0.0	316	421	0.99
17	22	241	388	388.0	4389	2364	2402	0.0	9	23	385	17394	31926	29173	0.0	267	425	0.99
17	25	241	387	389.4	8867	2414	2458	0.0	11	41	382	21980	34680	29245	0.0	356	434	0.99
17	27	241	385	389.0	2483	2570	2618	0.0	4	19	382	77815	36786	29298	0.0	1036	416	0.99
17	31	241	392	393.0	4195	3319	3404	0.0	13	28	445	232496	41893	29416	13.3	3600	470	1.14
17	35	241	397	402.0	32335	3531	3628	0.0	143	408	390	62163	48367	29550	0.3	3600	471	0.98
17	41	241	394	397.0	10248	9165	9280	0.0	132	294	607	65545	61041	29781	36.6	3600	490	1.54
17	49	241	394	398.0	5129	9574	9713	0.0	20	94	524	23990	84779	30145	26.7	3600	510	1.33
18	21	301	566	566.0	7527	3337	3392	0.0	11	20	558	5435	46087	45381	0.0	325	613	0.99
18	22	301	566	566.0	1199	3606	3664	0.0	2	11	558	12606	46824	45403	0.0	463	624	0.99
18	24	301	566	566.0	4220	3383	3447	0.0	10	23	558	10086	48415	45450	0.0	424	639	0.99
18	26	301	566	569.0	19255	3792	3864	0.0	61	86	562	81781	50828	45501	0.0	1922	642	0.99
18	28	301	567	570.0	6717	3349	3425	0.0	17	74	621	193951	53317	45556	11.6	3600	629	1.10
18	31	301	566	566.0	8137	3373	3458	0.0	22	213	554	81956	57307	45646	0.0	3233	644	0.98
18	34	301	573	576.6	5543	3588	3682	0.0	12	28	568	83856	62106	45745	3.2	3600	636	0.99
18	38	301	569	574.0	1867	3659	3765	0.0	7	29	764	93716	69755	45891	28.3	3600	670	1.34
18	43	301	576	581.8	3258	9607	9728	0.0	13	110	563	10279	81973	46096	2.5	3600	678	0.98
18	51	301	566	588.0	10806	9576	9721	0.0	64	193	566	6558	108039	46476	3.4	3600	707	1.00
18	61	301	587	600.0	14139	9548	9723	0.0	93	414	-	64	154177	47041	-	3600	739	-
19	25	361	899	908.0	49785	9525	9730	26.5	1889	3600	888	147472	67339	65305	1.8	3600	1012	0.99
19	26	361	934	934.0	50623	8476	8690	13.1	3593	3600	894	153976	68552	65331	2.7	3600	1041	0.96
19	28	361	765	767.0	12458	3221	3297	0.0	35	127	741	76185	71214	65386	0.0	3070	860	0.97
19	31	361	766	768.8	2781	3516	3601	0.0	7	24	916	90675	75856	65476	21.0	3600	873	1.20
19	33	361	739	744.0	3071	3760	3851	0.0	5	129	727	9636	79362	65541	0.0	3464	863	0.98
19	37	361	746	767.2	12686	4518	4656	0.0	70	260	798	18486	86959	65683	9.3	3600	893	1.07
19	41	361	769	773.4	7469	9557	9711	0.0	37	204	927	16062	96064	65841	22.0	3600	932	1.21
19	46	361	769	777.0	4524	9720	9894	0.0	27	203	735	6480	109938	66061	1.6	3600	929	0.96
19	52	361	780	791.0	13053	9633	9831	0.0	114	256	-	6370	131081	66358	-	3600	1014	-
19	61	361	774	785.4	9080	9419	9653	0.0	144	453	-	120	173470	66871	-	3600	1035	-
19	73	361	825	835.0	8746	9652	9934	0.0	120	228	-	1	253098	67681	-	3600	1050	-
Average(Table 5 & 6)					7084.1	5010.7	5100.3			72.0	146.7	79438.6	63824.4	41447.3	(35/110)	2881.0		1.04 (64/110)

obverse. However, the figure clearly shows that the number of nodes in SIM is consistently and significantly lower than that in the Exact. On average, the explored nodes in SIM are only 9 % of that in the Exact.

In Figure 10, we visualize the training data of a specific instance as a typical example. The training data in this figure exhibits a two-dimensional normal distribution. The optimal solution obtained by the SIM is located near the estimated line, suggesting that our theoretical approach applies to this problem. Figure 11 illustrates the comparison of the average of the minimum objective values obtained from different groups of case studies with the average objective values solved by the SIM. We can observe that the solutions derived from SIM consistently outperform the minimum values obtained from sampling. This also indicates that our framework exhibits certain learning capabilities in this problem.

The experimental data presented above demonstrates properties similar to those observed in Case I. Our framework is capable of generating models of limited size for this problem, which exhibit fewer explored nodes during the solving process. Furthermore, the outcomes display a notable difference with minimal

Table 7 The SIM in SoftCluVRP BKS and heuristic comparison (Part1)

Δ	Cluster	Customer	SIM(20s)			BKS †	LMNS			Ratio		
			Obj _{best}	Obj _{avg}	Time _{Total}		Obj _{best}	Obj _{avg}	Time _{Total}	BKS/SIM _{best}	(LMNS/SIM) _{best}	(LMNS/SIM) _{avg}
1	17	241	4640	4640.0	6	4640*	4640	4640.0	30	1.00	1.00	1.00
1	18	241	4652	4664.6	9	4645	4645	4645.0	31	1.00	1.00	1.00
1	19	241	4667	4685.0	10	4650	4650	4650.0	33	1.00	1.00	0.99
1	21	241	4669	4681.0	13	4650	4650	4650.0	33	1.00	1.00	0.99
1	22	241	4677	4694.0	25	4650	4650	4650.0	33	0.99	0.99	0.99
1	25	241	4660	4664.6	30	4650	4650	4651.2	35	1.00	1.00	1.00
1	27	241	4658	4663.4	23	4652	4652	4652.0	35	1.00	1.00	1.00
1	31	241	4710	4716.0	49	4665	4665	4665.0	44	0.99	0.99	0.99
1	35	241	4732	4740.2	58	4619	4619	4619.8	46	0.98	0.98	0.97
1	41	241	4685	4726.0	121	4619	4619	4621.3	44	0.99	0.99	0.98
1	49	241	4803	4860.4	117	4607	4619	4625.5	47	0.96	0.96	0.95
2	22	321	7442	7485.6	24	7394	7394	7395.9	66	0.99	0.99	0.99
2	23	321	7392	7403.2	46	7369*	7372	7381.2	66	1.00	1.00	1.00
2	25	321	7414	7426.2	24	7367	7367	7370.4	69	0.99	0.99	0.99
2	27	321	7399	7402.4	25	7333	7333	7334.3	72	0.99	0.99	0.99
2	30	321	7428	7445.0	36	7329	7329	7329.0	78	0.99	0.99	0.98
2	33	321	7443	7493.8	48	7311	7311	7314.1	80	0.98	0.98	0.98
2	36	321	7396	7494.2	38	7293	7293	7293.2	84	0.99	0.99	0.97
2	41	321	7385	7451.0	69	7283	7283	7286.2	88	0.99	0.99	0.98
2	46	321	7449	7541.8	71	7284	7284	7290.7	95	0.98	0.98	0.97
2	54	321	7560	7720.0	122	7274	7277	7278.7	101	0.96	0.96	0.94
2	65	321	7697	7780.0	115	7261	7264	7272.4	104	0.94	0.94	0.93
5	14	201	6970	6970.0	19	6970*	6970	6970.0	22	1.00	1.00	1.00
5	15	201	6933	6933.0	5	6742*	6742	6752.0	26	0.97	0.97	0.97
5	16	201	6895	6920.2	10	6742*	6742	6849.1	26	0.98	0.98	0.99
5	17	201	6862	6862.0	5	6862*	6862	6868.0	26	1.00	1.00	1.00
5	19	201	7030	7030.0	28	6874*	6874	6874.0	25	0.98	0.98	0.98
5	21	201	6881	6885.0	20	6816*	6816	6817.4	26	0.99	0.99	0.99
5	23	201	6887	6943.8	17	6750*	6750	6750.0	25	0.98	0.98	0.97
5	26	201	6880	6882.6	9	6704*	6704	6704.0	27	0.97	0.97	0.97
5	29	201	6879	6910.0	25	6704*	6704	6704.0	28	0.97	0.97	0.97
5	34	201	6833	7031.0	26	6684	6684	6692.4	29	0.98	0.98	0.95
5	41	201	7097	7128.2	125	6557*	6557	6578.2	32	0.92	0.92	0.92
6	19	281	8115	8122.2	14	8115*	8115	8115.3	54	1.00	1.00	1.00
6	21	281	8119	8134.4	7	8119*	8119	8125.5	52	1.00	1.00	1.00
6	22	281	8107	8107.0	15	8107*	8107	8113.7	52	1.00	1.00	1.00
6	24	281	8316	8351.0	8	8316*	8316	8318.8	52	1.00	1.00	1.00
6	26	281	8285	8305.0	25	8249*	8249	8256.4	54	1.00	1.00	0.99
6	29	281	8278	8320.8	91	8244	8244	8251.4	60	1.00	1.00	0.99
6	32	281	8486	8504.0	69	8179	8179	8197.3	59	0.96	0.96	0.96
6	36	281	8331	8470.6	52	8179	8179	8180.9	59	0.98	0.98	0.97
6	41	281	8595	8679.8	100	8204	8204	8206.5	66	0.95	0.95	0.95
6	47	281	8686	8770.0	104	8179	8179	8192.6	65	0.94	0.94	0.93
6	57	281	9059	9116.0	307	8204	8204	8205.6	75	0.91	0.91	0.90
7	25	361	9369	9461.6	20	9318	9318	9321.5	99	0.99	0.99	0.99
7	26	361	9536	9536.0	8	9295	9307	9314.1	101	0.97	0.98	0.98
7	28	361	9448	9521.2	17	9271	9272	9282.7	109	0.98	0.98	0.97
7	31	361	9667	9752.0	25	9418	9418	9442.6	101	0.97	0.97	0.97
7	33	361	9687	9731.0	37	9395	9401	9401.8	103	0.97	0.97	0.97
7	37	361	9764	9776.2	66	9395	9395	9403.7	104	0.96	0.96	0.96
7	41	361	9729	9747.2	106	9386	9386	9400.3	108	0.96	0.96	0.96
7	46	361	9685	9771.0	149	9368	9368	9376.7	102	0.97	0.97	0.96
7	52	361	9788	9890.0	184	9365	9365	9373.1	114	0.96	0.96	0.95
7	61	361	10140	10185.8	587	9316	9316	9343.6	128	0.92	0.92	0.92
7	73	361	9911	10076.2	143	9302	9302	9314.9	145	0.94	0.94	0.92
9	18	256	281	282.4	5	281*	281	281.0	39	1.00	1.00	1.00
9	19	256	283	283.0	16	279*	279	279.2	38	0.99	0.99	0.99
9	20	256	280	280.0	20	276*	276	276.6	40	0.99	0.99	0.99
9	22	256	276	278.0	18	276*	276	276.7	44	1.00	1.00	1.00
9	24	256	276	279.8	28	276*	276	276.9	44	1.00	1.00	0.99
9	26	256	278	279.6	35	273*	273	273.9	46	0.98	0.98	0.98
9	29	256	279	281.0	35	273*	273	273.6	45	0.98	0.98	0.97
9	32	256	284	286.4	57	273*	273	273.9	48	0.96	0.96	0.96
9	37	256	289	290.4	27	273	273	273.9	50	0.94	0.94	0.94
9	43	256	287	291.0	51	270	270	270.8	53	0.94	0.94	0.93
9	52	256	293	296.0	49	269	269	269.0	57	0.92	0.92	0.91

Table 8 The SIM in SoftCluVRP BKS and heuristic comparison (Part2)

Δ	Cluster	Customer	SIM(20s)			BKS \dagger	LMNS			Ratio		
			Obj _{best}	Obj _{avg}	Time _{total}		Obj _{best}	Obj _{avg}	Time _{total}	BKS/SIM _{best}	(LMNS/SIM) _{best}	(LMNS/SIM) _{avg}
13	17	253	535	535.0	12	530*	530	530.4	40	0.99	0.99	0.99
13	19	253	530	533.6	36	521*	521	521.8	40	0.98	0.98	0.98
13	20	253	532	532.0	37	521*	521	521.5	42	0.98	0.98	0.98
13	22	253	533	533.8	16	523*	523	523.2	42	0.98	0.98	0.98
13	23	253	533	533.0	24	523*	523	523.2	43	0.98	0.98	0.98
13	26	253	531	532.2	27	523*	523	523.0	46	0.98	0.98	0.98
13	29	253	534	537.0	28	522*	522	522.0	48	0.98	0.98	0.97
13	32	253	530	533.0	17	521*	521	521.2	49	0.98	0.98	0.98
13	37	253	533	537.8	41	521*	521	521.9	53	0.98	0.98	0.97
13	43	253	533	536.0	84	521	521	521.0	54	0.98	0.98	0.97
13	51	253	547	551.0	78	521	521	521.0	58	0.95	0.95	0.95
17	17	241	393	393.2	9	386*	386	386.0	44	0.98	0.98	0.98
17	18	241	393	393.0	8	385*	385	385.0	45	0.98	0.98	0.98
17	19	241	388	388.0	10	385*	385	385.0	46	0.99	0.99	0.99
17	21	241	388	388.0	15	385*	385	385.0	47	0.99	0.99	0.99
17	22	241	388	388.0	23	385*	385	385.0	47	0.99	0.99	0.99
17	25	241	387	389.4	41	382*	382	382.2	47	0.99	0.99	0.98
17	27	241	385	389.0	19	382*	382	382.0	49	0.99	0.99	0.98
17	31	241	392	394.8	24	390*	390	390.0	51	0.99	0.99	0.99
17	35	241	394	403.0	26	390	390	390.0	57	0.99	0.99	0.97
17	41	241	398	399.2	36	388	388	388.4	59	0.97	0.97	0.97
17	49	241	414	416.4	70	387	387	387.2	60	0.93	0.93	0.93
18	21	301	566	566.0	16	558*	558	558.0	58	0.99	0.99	0.99
18	22	301	566	566.0	11	558*	558	558.0	59	0.99	0.99	0.99
18	24	301	566	566.0	46	558*	558	558.0	64	0.99	0.99	0.99
18	26	301	573	574.8	58	562*	562	562.0	63	0.98	0.98	0.98
18	28	301	567	572.0	81	558	558	558.0	66	0.98	0.98	0.98
18	31	301	566	566.0	36	554*	554	554.0	71	0.98	0.98	0.98
18	34	301	577	578.2	35	554*	554	554.1	70	0.96	0.96	0.96
18	38	301	579	597.0	40	555	555	555.1	74	0.96	0.96	0.93
18	43	301	588	591.8	36	558	558	558.0	83	0.95	0.95	0.94
18	51	301	619	620.0	54	555	555	555.9	83	0.90	0.90	0.90
18	61	301	622	628.0	75	556	556	556.6	92	0.89	0.89	0.89
19	25	361	928	931.6	25	886*	887	887.9	50	0.95	0.96	0.95
19	26	361	931	933.8	48	888*	889	889.0	51	0.95	0.95	0.95
19	28	361	763	766.0	47	741*	741	742.0	77	0.97	0.97	0.97
19	31	361	763	769.2	36	735	737	737.5	84	0.96	0.97	0.96
19	33	361	759	766.0	70	727*	728	729.1	89	0.96	0.96	0.95
19	37	361	751	772.6	58	732*	733	733.5	100	0.97	0.98	0.95
19	41	361	778	783.8	53	730	730	730.7	109	0.94	0.94	0.93
19	46	361	778	785.0	71	730	730	730.7	115	0.94	0.94	0.93
19	52	361	781	801.0	91	730	730	730.8	120	0.93	0.93	0.91
19	61	361	790	830.8	104	737	737	738.5	120	0.93	0.93	0.89
19	73	361	801	827.0	130	736	736	736.9	135	0.92	0.92	0.89
Average(Table 7 & 8)					52.2				62.5	0.97	0.97	0.97

\dagger The BKS objective values attached with * are proved to be optimal by Hintsch and Irnich (2020)

sampling values, indicating a learning capacity. It is suggested we can attribute the improvements of the SIM to the modifications by our framework, as an answer to **Q3**.

Finally, we restrict the computation time for each surrogate model within the Algorithm 2 to 20 seconds. This approach is then compared with the best-known solution (BKS) as documented in Hintsch and Irnich (2020) and Hintsch (2021). Furthermore, a comparison is made with the latest state-of-the-art heuristic, referred to as LMNS in Hintsch (2021). The comparative outcomes are depicted in Tables 7 and 8. We can observe that the objective values of the SIM are closely aligned with those of the BKS and LMNS, with all differences being within 3% on average. Their results are almost equivalent for instances with no more than 30 clusters. Remarkably, the SIM demonstrated a superior average processing speed compared to the

LMNS. This competitive performance suggests that the SIM could be considered as generally practical for the medium-sized SoftCluVRP as a heuristic algorithm.

Figure 8 Scatter of model sizes

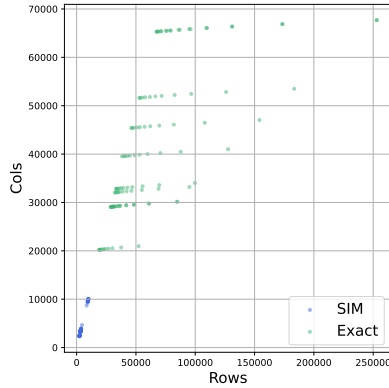


Figure 9 Explored nodes during the B&C process

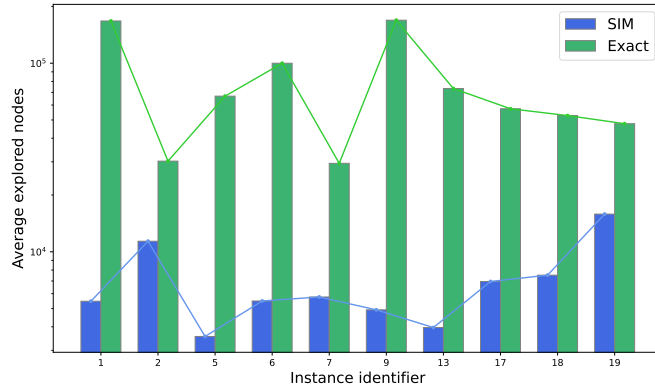


Figure 10 Parity plot of sampled data of the SIM and Exact models

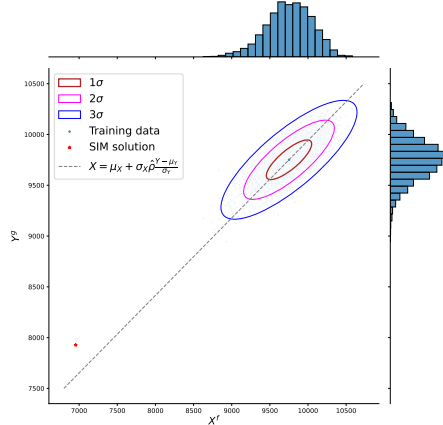
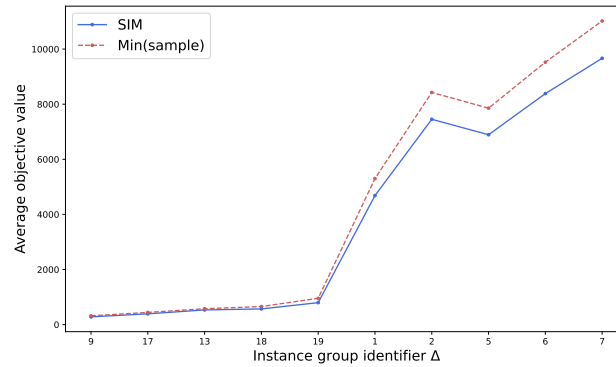


Figure 11 The comparison of average group objective values of the SIM the Min(sample)



6. Conclusion

This study concentrates on the GAPR and presents a framework to generate surrogate models, improving the efficiency of B&C-based problem-solving. To address the complexity involved by the routing constraints, we define a class of surrogate models to reduce decision variables and reconstruct constraints. We propose a framework for the learning of surrogate models through empirical data. Following this, the study provides theoretical insights concerning the representational power and statistical properties of the framework, yielding theoretical guarantees for its effectiveness. Experimental evaluations highlight the framework’s accuracy and improved efficiency across varying scales within two practical problem classes, compared with the exact formulations as its learning target. Moreover, the framework shows close or superior performance compared

with the state-of-the-art heuristics, providing supporting evidence on its general practicality, especially on small and medium problem sizes. Therefore, we can conclude that the proposed framework on the GAPR is effective in producing high-quality solutions with promoted efficiency.

In the future, the framework could be expanded to solve black-box optimization tasks. Furthermore, there is potential for integrating the framework with heuristic approaches or exact algorithms, serving as a warm start to facilitate the solution of complex problems.

Acknowledgments

This work was funded by the National Natural Science Foundation of China under Grant No. 12320101001 and 12071428.

References

- Aerts B, Cornelissens T, Sörensen K (2021) The joint order batching and picker routing problem: Modelled and solved as a clustered vehicle routing problem. *Computers & Operations Research* 129:105168.
- Anderson R, Huchette J, Ma W, Tjandraatmadja C, Vielma JP (2020) Strong mixed-integer programming formulations for trained neural networks. *Mathematical Programming* 183(1-2):3–39.
- Aringhieri R, Landa P, Soriano P, Tanfani E, Testi A (2015) A two level metaheuristic for the operating room scheduling and assignment problem. *Computers & Operations Research* 54:21–34.
- Azizian W, Lelarge M (2021) Expressive power of invariant and equivariant graph neural networks. *ICLR 2021-International Conference on Learning Representations*.
- Bartholdi JJ, Hackman ST (2014) Warehouse & distribution science: release 0.96. *The Supply Chain and Logistics Institute* 30332.
- Bengio Y, Lodi A, Prouvost A (2021) Machine learning for combinatorial optimization: a methodological tour d’horizon. *European Journal of Operational Research* 290(2):405–421.
- Benjaafar S, ElHafsi M, Vericourt Fd (2004) Demand allocation in multiple-product, multiple-facility, make-to-stock systems. *Management Science* 50(10):1431–1448.
- Bertsimas D, O’Hair A, Relyea S, Silberholz J (2016) An analytics approach to designing combination chemotherapy regimens for cancer. *Management Science* 62(5):1511–1531.
- Biggs M, Hariss R, Perakis G (2017) Optimizing objective functions determined from random forests. *Available at SSRN 2986630*.
- Boccia M, Masone A, Sterle C, Murino T (2023) The parallel agv scheduling problem with battery constraints: A new formulation and a matheuristic approach. *European Journal of Operational Research* 307(2):590–603.
- Cacchiani V, Salazar-González JJ (2017) Optimal solutions to a real-world integrated airline scheduling problem. *Transportation science* 51(1):250–268.

- Chen Z, Liu J, Wang X, Yin W (2022) On representing linear programs by graph neural networks. *The Eleventh International Conference on Learning Representations*.
- Cheng CY, Chen YY, Chen TL, Yoo JJW (2015) Using a hybrid approach based on the particle swarm optimization and ant colony optimization to solve a joint order batching and picker routing problem. *International Journal of Production Economics* 170:805–814.
- Defryn C, Sörensen K (2017) A fast two-level variable neighborhood search for the clustered vehicle routing problem. *Computers & Operations Research* 83:78–94.
- Dobson G, Nambimadom RS (2001) The batch loading and scheduling problem. *Operations research* 49(1):52–65.
- Fajemisin AO, Maragno D, den Hertog D (2023) Optimization with constraint learning: a framework and survey. *European Journal of Operational Research* .
- Fischetti M, Jo J (2018) Deep neural networks and mixed integer linear optimization. *Constraints* 23(3):296–309.
- Fischetti M, Ljubić I, Sinnl M (2016) Benders decomposition without separability: A computational study for capacitated facility location problems. *European Journal of Operational Research* 253(3):557–569.
- Gasse M, Chételat D, Ferroni N, Charlin L, Lodi A (2019) Exact combinatorial optimization with graph convolutional neural networks. *Advances in neural information processing systems* 32.
- Grimstad B, Andersson H (2019) Relu networks as surrogate models in mixed-integer linear programs. *Computers & Chemical Engineering* 131:106580.
- Gutiérrez-Sánchez A, Rocha-Medina LB (2022) Vrp variants applicable to collecting donations and similar problems: A taxonomic review. *Computers & Industrial Engineering* 164:107887.
- Gutina D, Bärmann A, Roeder G, Schellenberger M, Liers F (2023) Optimization over decision trees: a case study for the design of stable direct-current electricity networks. *Optimization and Engineering* 1–41.
- Halilbašić L, Thams F, Venzke A, Chatzivasileiadis S, Pinson P (2018) Data-driven security-constrained ac-opf for operations and markets. *2018 power systems computation conference (PSCC)*, 1–7 (IEEE).
- Härdle W, Simar L, et al. (2007) *Applied multivariate statistical analysis*, volume 22007 (Springer Berlin Heidelberg).
- Heßler K, Irnich S (2021) A branch-and-cut algorithm for the soft-clustered vehicle-routing problem. *Discrete Applied Mathematics* 288:218–234.
- Hintsch T (2021) Large multiple neighborhood search for the soft-clustered vehicle-routing problem. *Computers & Operations Research* 129:105132.
- Hintsch T, Irnich S (2020) Exact solution of the soft-clustered vehicle-routing problem. *European Journal of Operational Research* 280(1):164–178.
- Karimi-Mamaghan M, Mohammadi M, Meyer P, Karimi-Mamaghan AM, Talbi EG (2022) Machine learning at the service of meta-heuristics for solving combinatorial optimization problems: A state-of-the-art. *European Journal of Operational Research* 296(2):393–422.

- Khalil EB, Bodic PL, Song L, Nemhauser G, Dilkina B (2016) Learning to branch in mixed integer programming. *Proceedings of the Thirtieth AAAI Conference on Artificial Intelligence*, 724–731.
- Kilwein Z, Jalving J, Eydenberg M, Blakely L, Skolfield K, Laird C, Boukouvala F (2023) Optimization with neural network feasibility surrogates: Formulations and application to security-constrained optimal power flow. *Energies* 16(16):5913.
- Kleijnen JP (2018) *Design and analysis of simulation experiments* (Springer).
- Li J, Huang R, Dai JB (2017) Joint optimisation of order batching and picker routing in the online retailer’s warehouse in china. *International Journal of Production Research* 55(2):447–461.
- Lin CC, Kang JR, Hou CC, Cheng CY (2016) Joint order batching and picker manhattan routing problem. *Computers & Industrial Engineering* 95:164–174.
- Maniezzo V, Boschetti MA, Stützle T (2021) *Matheuristics: Algorithms and Implementations* (Springer International Publishing), ISBN 9783030702779.
- Matusiak M, De Koster R, Saarinen J (2017) Utilizing individual picker skills to improve order batching in a warehouse. *European Journal of Operational Research* 263(3):888–899.
- Mikić M, Todosijević R, Urošević D (2019) Less is more: General variable neighborhood search for the capacitated modular hub location problem. *Computers & Operations Research* 110:101–115.
- Mišić VV (2020) Optimization of tree ensembles. *Operations Research* 68(5):1605–1624.
- Mistry M, Letsios D, Krennrich G, Lee RM, Misener R (2021) Mixed-integer convex nonlinear optimization with gradient-boosted trees embedded. *INFORMS Journal on Computing* 33(3):1103–1119.
- Pardo EG, Gil-Borrás S, Alonso-Ayuso A, Duarte A (2024) Order batching problems: Taxonomy and literature review. *European Journal of Operational Research* 313(1):1–24.
- Paulus MB, Zarpellon G, Krause A, Charlin L, Maddison C (2022) Learning to cut by looking ahead: Cutting plane selection via imitation learning. *International conference on machine learning*, 17584–17600 (PMLR).
- Pentico DW (2007) Assignment problems: A golden anniversary survey. *European Journal of Operational Research* 176(2):774–793.
- Rigo CA, Seman LO, Morsch Filho E, Camponogara E, Bezerra EA (2023) Mippt aware task scheduling for nanosatellites using mip-based relu proxy models. *Expert Systems with Applications* 234:121022.
- Schweidtmann AM, Bongartz D, Mitsos A (2022) Optimization with trained machine learning models embedded. *Encyclopedia of Optimization*, 1–8 (Springer).
- Sevaux M, Sörensen K (2008) Hamiltonian paths in large clustered routing problems. *workshop on Metaheuristics for Logistics and Vehicle Routing, EU/ME’08*, 411–417.
- Taillard É, Badeau P, Gendreau M, Guertin F, Potvin JY (1997) A tabu search heuristic for the vehicle routing problem with soft time windows. *Transportation science* 31(2):170–186.

- Valle CA, Beasley JE (2020) Order batching using an approximation for the distance travelled by pickers. *European Journal of Operational Research* 284(2):460–484.
- Valle CA, Beasley JE, da Cunha AS (2016) Modelling and solving the joint order batching and picker routing problem in inventories. *Combinatorial Optimization: 4th International Symposium, ISCO 2016, Vietri sul Mare, Italy, May 16-18, 2016, Revised Selected Papers 4*, 81–97 (Springer).
- Valle CA, Beasley JE, Da Cunha AS (2017) Optimally solving the joint order batching and picker routing problem. *European Journal of Operational Research* 262(3):817–834.
- Van Gils T, Ramaekers K, Caris A, De Koster RB (2018) Designing efficient order picking systems by combining planning problems: State-of-the-art classification and review. *European journal of operational research* 267(1):1–15.
- Wang K, Lozano L, Cardonha C, Bergman D (2023) Optimizing over an ensemble of trained neural networks. *INFORMS Journal on Computing* 35(3):652–674.
- Won J, Olafsson* S (2005) Joint order batching and order picking in warehouse operations. *International journal of production research* 43(7):1427–1442.
- Wu Y, Song W, Cao Z, Zhang J (2021) Learning large neighborhood search policy for integer programming. *Advances in Neural Information Processing Systems* 34:30075–30087.
- Yadav N, Tanksale A (2022) An integrated routing and scheduling problem for home healthcare delivery with limited person-to-person contact. *European Journal of Operational Research* 303(3):1100–1125.
- Zhang J, Liu C, Li X, Zhen HL, Yuan M, Li Y, Yan J (2023) A survey for solving mixed integer programming via machine learning. *Neurocomputing* 519:205–217.
- Zhang K, Gao C (2023) Improved formulations of the joint order batching and picker routing problem. *International Journal of Production Research* 61(21):7386–7409.
- Zhou J, Shi T, Ren J, He C (2024) Accelerating operation optimization of complex chemical processes: A novel framework integrating artificial neural network and mixed-integer linear programming. *Chemical Engineering Journal* 481:148421.
- Zou H, Hastie T, Tibshirani R (2007) On the “degrees of freedom” of the lasso. *The Annals of Statistics* 35(5):2173–2192.